

RSC Advances



This is an *Accepted Manuscript*, which has been through the Royal Society of Chemistry peer review process and has been accepted for publication.

Accepted Manuscripts are published online shortly after acceptance, before technical editing, formatting and proof reading. Using this free service, authors can make their results available to the community, in citable form, before we publish the edited article. This *Accepted Manuscript* will be replaced by the edited, formatted and paginated article as soon as this is available.

You can find more information about *Accepted Manuscripts* in the [Information for Authors](#).

Please note that technical editing may introduce minor changes to the text and/or graphics, which may alter content. The journal's standard [Terms & Conditions](#) and the [Ethical guidelines](#) still apply. In no event shall the Royal Society of Chemistry be held responsible for any errors or omissions in this *Accepted Manuscript* or any consequences arising from the use of any information it contains.

ARTICLE

Facile hydrothermal synthesis of SnO₂/C microspheres and double layered core-shell SnO₂ microspheres as anode materials for Li-ion secondary batteries

Cite this: DOI: 10.1039/x0xx00000x

Received 00th January 2012,
Accepted 00th January 2012

DOI: 10.1039/x0xx00000x

www.rsc.org/

Mingbo Wu,^{*a} Jun Liu,^a Minghui Tan,^a Zhongtao Li,^a Wenting Wu,^a Yanpeng Li,^a Huaiping Wang,^a Jingtang Zheng,^a and Jieshan Qiu,^{*b}

SnO₂/C microspheres and double layered core-shell SnO₂ microspheres have been synthesized by a facile hydrothermal method with a post heat-treatment. The soluble starch used as carbon source and the mass ratio of starch to SnCl₄•5H₂O play key roles in the formation of SnO₂/C microspheres, and the hydrothermal synthesis mechanism of SnO₂/C microspheres has been proposed. SnO₂/C-1.0 microspheres (the mass ratio of soluble starch to SnCl₄•5H₂O is 1:1) with good spherical shape and 34.91 wt% of SnO₂ exhibit superior rate capability and cyclic stability, while double layered core-shell SnO₂ microspheres show improved electrochemical performances than SnO₂ particles. The electrode based on SnO₂/C-1.0 microspheres delivers a reversible discharge capacity of 568 mAh/g at a constant current density of 100 mA/g in the second cycle, and 379 mAh/g (67% retention) is retained after the 50th cycle, suggesting SnO₂/C microspheres a promising candidate for energy storage.

1 Introduction

Li-ion batteries (LIBs) have attracted significant attention due to their high work voltage, high energy density, high energy efficiency, long cycle life and environmentally friendly nature.¹⁻³ Such outstanding advantages make them good candidates for applications in hybrid electric vehicles, portable electronics, large industrial equipments, and other renewable energy storages.^{1, 3, 4} The electrochemical properties of LIBs largely depend on their electrode materials, currently used commercial graphite anodes have a limited theoretical capacity of 372 mAh/g, so alternative materials are highly desired.^{3, 5, 6}

SnO₂ as LIBs anode has attracted much attention on the basis of its higher theoretical specific capacity (790 mAh/g) than that of graphite.^{7, 8} However, a large volume change (about 300%) occurs in SnO₂ anode during lithium insertion/extraction processes, which causes pulverization of anode particles and loss of contact with current collector, resulting in poor electrochemical performance.^{5, 7-9} In order to improve the electrochemical properties of SnO₂-based anodes, lots of effective ways to regulate the composition or structure of the electrode material have been reported. SnO₂/carbon composites,^{10, 11} hollow or core-shell SnO₂/carbon composites,^{7, 12, 13} SnO₂/graphene composites,¹⁴⁻¹⁸ and hollow or yolk-shell SnO₂ spheres^{8, 9, 19-22} have been prepared and used as anode materials for LIBs in recent years. Although all of above mentioned SnO₂-based materials have improved electrochemical properties, the complex technologies or tedious multi-step methods used in their preparation process hinder their widely industrial applications.

In this work, a facile hydrothermal method of synthesizing SnO₂/C microspheres and double layered core-shell SnO₂ microspheres with a post heat-treatment was proposed. The mechanism of the hydrothermal formation of SnO₂/C microspheres was discussed, and the electrochemical performances of SnO₂/C microspheres and core-shell-structured SnO₂ microspheres in LIBs were investigated.

2 Experimental

2.1 Sample preparation

The overall synthetic procedure is described in Fig. 1. SnCl₄•5H₂O (AR, Sinopharm Chemical Reagent Co., Ltd.) and soluble starch (AR, Sinopharm Chemical Reagent Co., Ltd.) were selected as the precursors of SnO₂ and carbon material, respectively. Soluble starch and SnCl₄•5H₂O were fully dispersed in deionized water with the mass ratio of soluble starch, SnCl₄•5H₂O and water at 1:1:3.37. 80 mL of the resulting mixture was transferred into a 100 mL Teflon-lined stainless steel autoclave, and then heated at 190 °C for 12 h. Dark precipitates were collected and washed with distilled water and ethanol, and finally dried in an oven at 100 °C for 12 h, thus, primary SnO₂/C microspheres were obtained. The primary SnO₂/C microspheres were then carbonized at 500 °C for 3 h under nitrogen atmosphere to prepare SnO₂/C microspheres (named SnO₂/C-1.0). For the preparation of core-shell-structured SnO₂ microspheres, the primary SnO₂/C microspheres were calcined in air at 600 °C for 3 h.

2.2 Characterization of samples

The surface morphology and microstructure of obtained samples were investigated by field emission scanning electron microscopy (FE-SEM, S4800, Japan) and transmission electron microscopy (TEM, JEM-2100UHR, Japan). The phase composition and crystalline properties of as-prepared products were characterized by X-ray diffraction (XRD, X'Pert PRO MPD, Netherlands).

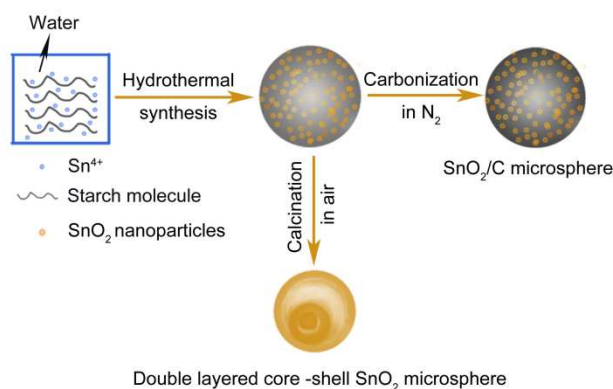


Fig. 1 Schematic formation processes of SnO_2/C microspheres and double layered core-shell SnO_2 microspheres

2.3 Preparation of electrodes and electrochemical measurements

The obtained sample was mixed with carbon black and polyvinylidene fluoride (PVDF) binder to form slurry at the weight ratio of 8:1:1. N-methyl-2-pyrrolidone was used as the solvent. The electrode was prepared by casting the slurry onto copper foil and drying in a vacuum oven at 120 °C for 12 h. CR2032 coin cells were assembled in an Ar-filled glove-box with lithium foil as the counter electrode, and polypropylene film (Celgard 2400) as the separator. The electrolyte was 1 M LiPF_6 dissolved in 1:1 volume ratio with ethylene carbonate/dimethyl carbonate (EC/DMC). The electrochemical properties of the electrodes were studied by cyclic voltammetry and galvanostatic charge-discharge on Arbin battery test system (BT2000, Arbin Instruments, USA). Cyclic voltammetry was performed in the potential range from 0.01 to 3 V (vs. Li^+/Li) at a scan rate of 0.2 mV/s. Galvanostatic charge-discharge measurements were carried out between 0.01 and 3 V (vs. Li^+/Li) at different current densities.

3 Results and discussion

Fig. 2 shows the XRD patterns of SnO_2/C -1.0 microspheres and double layered core-shell SnO_2 microspheres. The pattern of double layered core-shell SnO_2 microspheres can be indexed well as SnO_2 . The four dominant broad peaks (110), (101), (211), and (301) in XRD pattern of double layered core-shell SnO_2 microspheres are attributed to the SnO_2 phase (JCPDS No. 41-1445), indicating the formation of tetragonal SnO_2 nanocrystals. Some weak peaks of metallic Sn are exhibited in the XRD pattern of SnO_2/C -1.0 microspheres, indicating little

amount of SnO_2 were reduced to metallic Sn by carbon during the heat-treated process.¹⁰

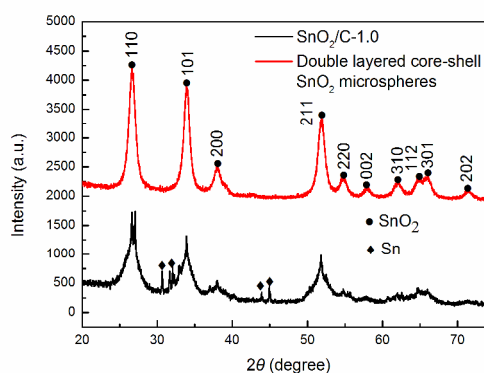


Fig. 2 XRD patterns of SnO_2/C -1.0 microspheres and double layered core-shell SnO_2 microspheres

From SEM images shown in Fig. 3(A) and (B), we can see that SnO_2/C -1.0 microspheres are mainly in spherical shape with particle size ranging from 1 to 5 μm , and the spheres are solid. Energy dispersive spectrometer (EDS, S4800, Japan) analysis was used to evaluate the composition of the smaller particles in Fig. 3(A), Sn, O and C are found in the smaller particles (see Fig. S1 in the Supporting Information), implying that the smaller particles are the composite of SnO_2 and carbon. Double layered core-shell SnO_2 microspheres in Fig. 3(C) are distinctly smaller than SnO_2/C -1.0 microspheres in Fig. 3(A) and there is an open hole on the surface of most double layered core-shell SnO_2 microsphere, which was brought by the burning of carbon and polymeric molecules in air and inner gases were evacuated during calcination process.^{19, 21} Through the hole (Fig. 3(D)), we can clearly see that the microsphere is composed of a thin outer shell and an inside smaller sphere, indicating the core-shell structure of double layered core-shell SnO_2 microsphere.

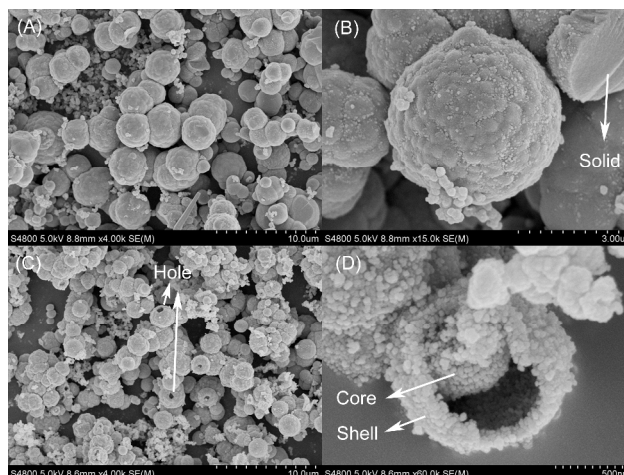


Fig. 3 SEM images of SnO_2/C -1.0 microspheres (A, B) and double layered core-shell SnO_2 microspheres (C, D)

TEM image in Fig. 4(A) shows that SnO_2/C -1.0 microspheres are solid spheres and SnO_2 nanoparticles are

uniformly dispersed in carbon matrix. Fig. 4(B) reveals the double layered core-shell structure of double layered core-shell SnO₂ microspheres. The high resolution TEM (HR-TEM) image of double layered core-shell SnO₂ microspheres, as shown in Fig. 4(C), exhibits clear lattice fringes separated by 0.33 nm and 0.26 nm, which are in good agreement with the (110) and (101) planes of rutile SnO₂, respectively. The corresponding ring-like selected-area electron diffraction (SAED) pattern shown in Fig. 4(D) indicates that the double layered core-shell SnO₂ microspheres are polycrystalline, and the diffraction rings of the pattern can be completely indexed to planes of rutile SnO₂, which also can be seen from XRD pattern in Fig. 2.

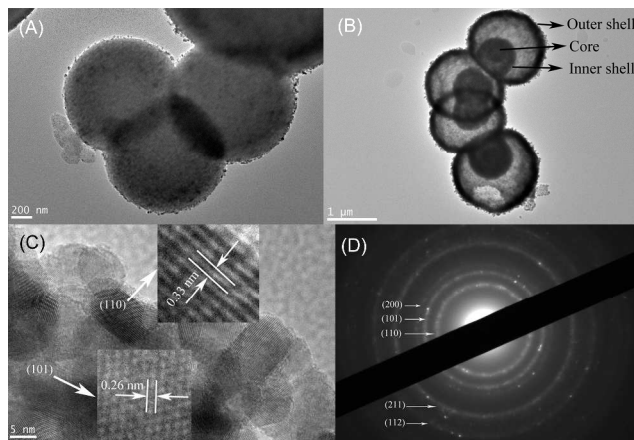


Fig. 4 TEM images of SnO₂/C-1.0 microspheres (A) and double layered core-shell SnO₂ microspheres (B), HR-TEM image (C) and SAED pattern (D) of double layered core-shell SnO₂ microsphere

The N₂ adsorption-desorption isotherms and pore size distribution of SnO₂/C-1.0 microspheres, double layered core-shell SnO₂ microspheres and SnO₂ particles prepared without starch are shown in Fig. S2 (see the Supporting Information). Fig. S2(A) shows that SnO₂/C-1.0 microspheres are microporous carbon evidenced by the type I isotherm while the pores in double layered core-shell SnO₂ microspheres and SnO₂ particles are mainly mesopores seen from the obvious hysteresis loops, which also can be clearly confirmed by the pore size distribution in Fig. S2(B). The BET surface area of SnO₂/C-1.0 microspheres, double layered core-shell SnO₂ microspheres and SnO₂ particles is 263 m²/g, 46 m²/g and 24 m²/g, respectively.

To evaluate the weight percentage of SnO₂ in SnO₂/C-1.0, the as-synthesized composite was calcined in air at 600 °C for 3 h, the obtained powders were white, indicating the carbon had been completely burned out and the residue was SnO₂. Thus the content of SnO₂ in SnO₂/C-1.0 microspheres is calculated to be 34.91 wt%. For comparison with SnO₂/C-1.0 microspheres (the mass ratio of soluble starch, SnCl₄·5H₂O and water was 1:1:3.37), SnO₂/C composites were prepared with the mass ratios of soluble starch, SnCl₄·5H₂O and water at 1:1.5:3.37 and 1:0.5:3.37, which were termed as SnO₂/C-1.5 and SnO₂/C-0.5, respectively. The contents of SnO₂ in SnO₂/C-1.5 and SnO₂/C-0.5 are about 34.62 wt% and 39.25 wt%, respectively. It is

interesting that the content of SnO₂ in SnO₂/C decreases with the increasing amount of added SnCl₄·5H₂O, more work is needed in future to explain this trend. From the SEM images of SnO₂/C-1.5 and SnO₂/C-0.5 (see Fig. S3 in the Supporting Information), we can see that both SnO₂/C-1.5 and SnO₂/C-0.5 show bad spherical shapes, indicating that there is a limitation of the amount of SnCl₄·5H₂O added and a suitable weight percentage of SnO₂ to keep the microsphere morphology.

To understand the role of starch molecule in the hydrothermal synthesis process of SnO₂/C microspheres, primary carbon microspheres and SnO₂ particles were obtained by the same hydrothermal method. The synthesis procedure of primary carbon microspheres or SnO₂ particles was as same as that of primary SnO₂/C microspheres except without addition of SnCl₄·5H₂O or soluble starch. From SEM images of the primary carbon microspheres (Fig. 5(A)) and the primary SnO₂/C microspheres (Fig. 5(B)), we can clearly see that the primary carbon microspheres have relatively smooth surface while primary SnO₂/C microspheres have raspberry-like surface, which may be due to the SnO₂ nanoparticles bedded in the primary SnO₂/C microspheres, see TEM image in Fig. 5(C). Fig. 5(D) shows the primary SnO₂ particles synthesized without addition of soluble starch, irregular aggregation of nanoparticles is observed and no obvious microsphere was obtained, implying the starch molecules do play an important role in the formation of SnO₂/C microspheres.

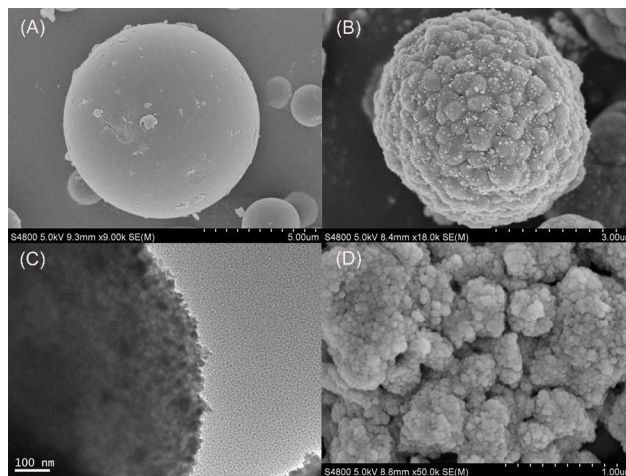


Fig. 5 SEM images of the primary carbon microsphere (A), the primary SnO₂/C microsphere (B) and primary SnO₂ particles (D) and TEM image of the primary SnO₂/C microsphere (C)

Hydrothermal synthesis mechanism of carbon microsphere from saccharides (starch,²³⁻²⁵ cellulose,²⁶ sucrose,^{23, 24} glucose,^{23, 24, 27} fructose²⁷) have been reported in references. Based on these references and our experimental results, we propose a possible hydrothermal synthesis mechanism of SnO₂/C microspheres, as show in Fig. 6. In the initial stage, the starch hydrolyzes and glucose molecules are produced. At the same time, hydrolysis of SnCl₄·5H₂O results in numerous primary SnO₂ hydrate nanoparticles in solution, and these SnO₂ hydrate nanoparticles are immediately entrapped by glucose molecules due to OH groups on glucose molecules.^{19, 25, 28} The

glucose molecules adsorbed on the surface of SnO₂ nanoparticles prevent the direct contact among SnO₂ nanoparticles, thus aggregation of SnO₂ nanoparticles is avoided. Driven by the reduction of overall surface energy, SnO₂ nanoparticles entrapped by glucose molecules aggregate to form microspheres.^{28, 29} In the hydrothermal environment, dehydration and polymerization reactions can take place among glucose molecules, thus the primary SnO₂/C microspheres are formed. As for the formation mechanism of double layered core-shell SnO₂ microspheres, the burning of carbon and polymeric molecules in air at 600 °C and the evacuation of inner gases during calcination process make the core-shell structure of double layered core-shell SnO₂ microspheres.^{20, 21}

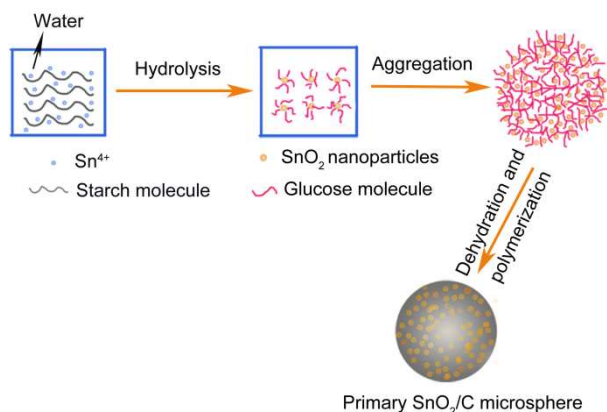
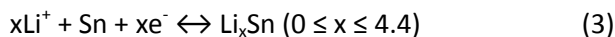
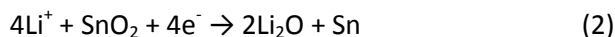
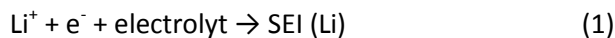


Fig. 6 Hydrothermal synthesis mechanism of SnO₂/C microspheres

Fig. 7 shows the initial 5 cyclic voltammograms of electrodes prepared from SnO₂/C-1.0 microspheres and double layered core-shell SnO₂ microspheres at a scan rate of 0.2 mV/s between 0.01 and 3 V. Two reduction peaks are observed in the first cathodic scan in both Fig. 7(A) and (B). The cathodic peaks around 0.6 V can be attributed to the formation of the solid electrolyte interface (SEI) layer and the reduction of SnO₂ to form Sn and Li₂O, the peak at low potential (< 0.5 V) corresponds to the formation of Li-Sn alloy,^{20, 30-32} the reactions as follows:



The oxidation peak at 0.54 V can be assigned to the de-alloying of Li_xSn, while the weak oxidation at 1.25 V is due to the partly reversible reaction (2). The obvious difference between the first cycle and the second cycle is due to irreversible reactions (1) and (2), leading to initially irreversible capacity loss.^{13, 15} From the 2nd cycle to the 5th cycle, the curves of SnO₂/C-1.0 microspheres become similar, suggesting better stability of SnO₂/C-1.0 microspheres than that of double layered core-shell SnO₂ microspheres.

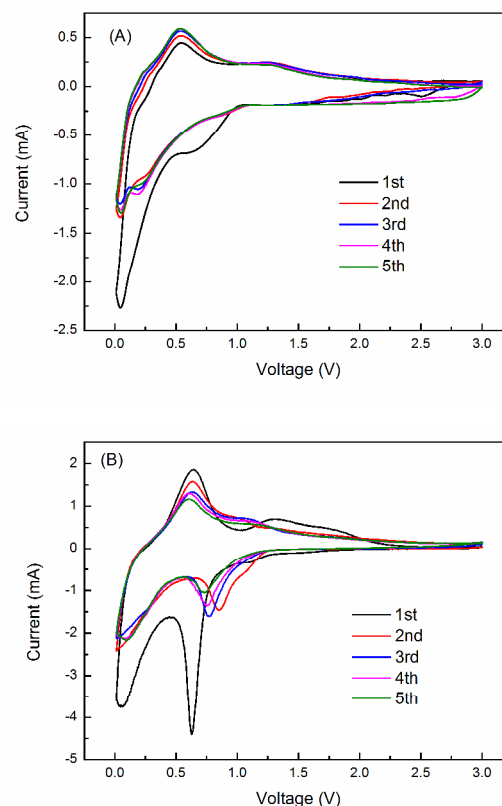


Fig. 7 Cyclic voltammograms of SnO₂/C-1.0 (A) and double layered core-shell SnO₂ microspheres (B)

For comparison, above mentioned primary SnO₂ particles were calcined in air at 600 °C for 3 h, and the obtained SnO₂ particles were used as anode material for LIBs. The cycling performances and rate capabilities of SnO₂/C-1.0 microspheres, double layered core-shell SnO₂ microspheres and SnO₂ particles are shown in Fig. 8(A) and (B), respectively. In Fig. 8(A), SnO₂/C-1.0 microspheres, double layered core-shell SnO₂ microspheres and SnO₂ particles deliver reversible discharge capacities of 568 mAh/g, 935 mAh/g, 825 mAh/g at a constant current density of 100 mA/g in the 2nd cycle, respectively, which are much higher than the theoretical capacity of graphite (372 mAh/g). The big initial irreversible capacity loss in the 1st cycle is due to the formation of the SEI layer and the reduction of SnO₂ to form Sn and Li₂O.^{10, 12, 20, 33} The higher capacities of double layered core-shell SnO₂ microspheres and SnO₂ particles than 790 mAh/g of the theoretical value can be attributed to the reversible polymerization of electrolyte^{9, 34} and the partly reversible reaction (2). The higher capacity of double layered core-shell SnO₂ microspheres than that of SnO₂ particles may be due to the increased contact area between the electrolyte and the electrode of the core-shell structure. Double layered core-shell SnO₂ microspheres and SnO₂ particles have high capacities in the initial several cycles, but the capacity decreases quickly due to pulverization of electrode materials.^{33, 35} The discharge capacities of double layered core-shell SnO₂ microspheres and SnO₂ particles after 50 cycles are 75 mAh/g

with capacity retention of 8% and 35 mAh/g with capacity retention of only 4%, respectively. The electrode produced from SnO₂/C-1.0 microspheres exhibits the best cycling performance, and its discharge capacity after 50 cycles is 379 mAh/g, 67% retention of the discharge capacity of the 2nd cycle. Fig. S4 (see the Supporting Information) gives the cycling performance of purely carbon microspheres, which deliver a reversible discharge capacity of only 116 mAh/g at a constant current density of 100 mA/g in the 2nd cycle, and 114 mAh/g is retained in the 50th cycle. So the high capacity of SnO₂/C-1.0 microspheres mainly comes from the SnO₂ component rather than the carbon. The coulombic efficiency of SnO₂/C-1.0 electrode is found to be around 93% for the second cycle and reaches above 98% for the 50th cycle. It is believed that carbon in SnO₂/C composite can buffer the big volume change during the charge and discharge processes and thereby enhance the structural stability of electrode.^{5, 10, 33, 36, 37, 38}

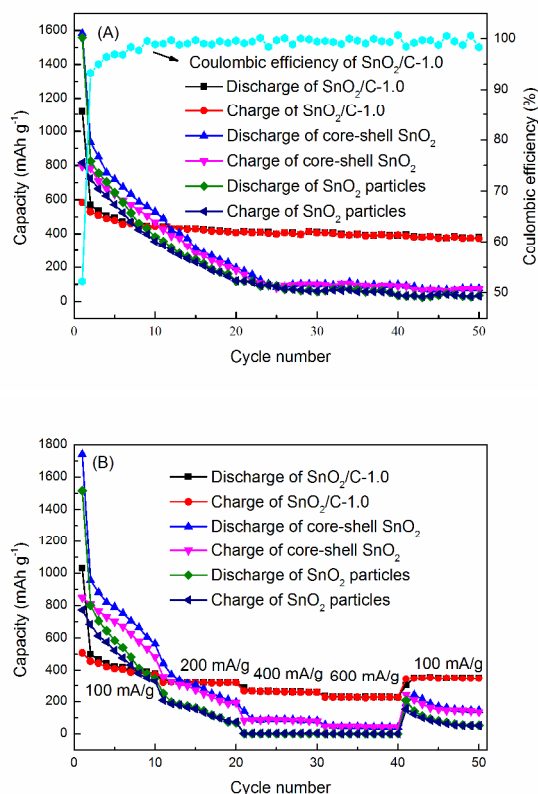


Fig. 8 The cycling performances (A) and rate capabilities (B) of the electrodes

In order to make sure the difference in the electrochemical performance of composites with different SnO₂ content, the electrochemical performances of SnO₂/C-1.5 and SnO₂/C-0.5 are shown in Fig. S5 (see the Supporting Information). SnO₂/C-1.5 and SnO₂/C-0.5 deliver reversible discharge capacities of 156 mAh/g and 419 mAh/g at a constant current density of 100 mA/g in the second cycle, respectively. After 50 cycles, SnO₂/C-1.5 and SnO₂/C-0.5 show stable discharge capacities of 154 mAh/g and 367 mAh/g. In comparison to SnO₂/C-1.5, the higher capacity of SnO₂/C-0.5 is due to its higher SnO₂ content

(the theoretical capacity of SnO₂ is 790 mAh/g). It is noted that the specific capacities of SnO₂/C-1.5 and SnO₂/C-0.5 are both lower than that of SnO₂/C-1.0 microspheres, while the SnO₂ content is SnO₂/C-0.5 > SnO₂/C-1.0 > SnO₂/C-1.5. The highest capacity of SnO₂/C-1.0 microspheres should be attributed to its good spherical shapes and suitable SnO₂ content.

Fig. 8(B) shows the capacity retention of electrodes at various current densities. Double layered core-shell SnO₂ microspheres have higher capacities than that of SnO₂ particles at all current densities, which results from the core-shell structure increasing contact area between the electrolyte and the electrode. The voids between core and shell can serve as a buffering space during lithium insertion and extraction processes.^{20, 22, 39} It is noted that the capacities of double layered core-shell SnO₂ microspheres at higher current densities are much lower than those of SnO₂/C-1.0 microspheres, indicating the worse stability of double layered core-shell SnO₂ microspheres than that of SnO₂/C-1.0 microspheres. At the current density of 100 mA/g, the capacity of SnO₂/C-1.0 microspheres is 378 mAh/g, and keeps 320 mAh/g, 260 mAh/g and 230 mAh/g at the current densities of 200 mA/g, 400 mA/g and 600 mA/g, respectively. When the current density switches back to 100 mA/g, the capacity directly recovers to 347 mAh/g, indicating excellent rate capability of SnO₂/C-1.0 microspheres.

Morphology changes of electrodes prepared from SnO₂/C-1.0 microspheres and double layered core-shell SnO₂ microspheres after 50 cycles at the current density of 100 mA/g are shown in Fig. 9. Most SnO₂/C-1.0 microspheres in Fig. 9(A) still keep good spherical shape as a whole integration structure, demonstrating that the carbon matrix can effectively accommodate the volume change and alleviate the strain during the charge and discharge processes. However, no spheres except many pulverized particles can be observed in the SEM image of electrode based on core-shell SnO₂ microspheres (see Fig. 9(B)), suggesting the obvious pulverization of double layered core-shell SnO₂ microspheres during the charge and discharge processes. The morphology changes shown in Fig. 9 can explain the better cycling performance of SnO₂/C-1.0 microspheres than that of double layered core-shell SnO₂ microspheres.

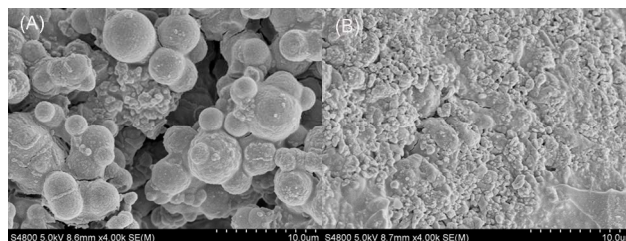


Fig. 9 SEM images of electrodes based on SnO₂/C-1.0 microspheres (A) and double layered core-shell SnO₂ microspheres (B) after 50 cycles at the current density of 100 mA/g

4 Conclusions

In conclusion, SnO₂/C microspheres and double layered core-shell SnO₂ microspheres have been synthesized by a facile hydrothermal method with a post heat-treatment. The soluble

starch used as the carbon source plays a key role in the formation of spherical SnO₂/C microspheres, and the hydrothermal mechanism of the formation of SnO₂/C microspheres has been proposed. Due to the barrier and buffer roles of carbon matrix, SnO₂/C microspheres exhibit superior rate capability and cyclic stability. The core-shell structured SnO₂ microspheres show improved electrochemical performances than SnO₂ particles, while their rate capability and cyclic stability are much worse than those of SnO₂/C microspheres. Therefore, SnO₂ nanoparticles in carbon matrix can effectively prevent the aggregation and pulverization of SnO₂ nanoparticles. It is noted that SnO₂/C microspheres in large scale can be easily prepared by this hydrothermal method, SnO₂/C microspheres may have good application future in the field of energy. This research work also can guide the preparation of metal oxide/carbon composites.

Acknowledgements

This work was supported by the National Natural Science Foundation of China (Nos.51172285, 51372277); the Fundamental Research Funds for the Central Universities (14CX06045A, 14CX02060A).

Notes and references

^a State Key Laboratory of Heavy Oil Processing, China University of Petroleum, Qingdao 266580, China. E-mail: wumb@upc.edu.cn.

^b Carbon Research Laboratory, State Key Lab of Fine Chemicals, School of Chemical Engineering, Dalian University of Technology, Dalian 116024, China. E-mail: jqiu@dlut.edu.cn

- N. S. Choi, Z. Chen, S. A. Freunberger, X. Ji, Y. K. Sun, K. Amine, G. Yushin, L. F. Nazar, J. Cho and P. G. Bruce, *Angew. Chem., Int. Ed.*, 2012, **51**, 9994-10024.
- P. Simon and Y. Gogotsi, *Nat. Mater.*, 2008, **7**, 845-854.
- M. V. Reddy, G. V. S. Rao and B. V. R. Chowdari, *Chem. Rev.*, 2013, **113**, 5364-5457.
- A. Manthiram, Y. Fu and Y.-S. Su, *Acc. Chem. Res.*, 2013, **46**, 1125-1134.
- Y. Xu, Q. Liu, Y. Zhu, Y. Liu, A. Langrock, M. R. Zachariah and C. Wang, *Nano Lett.*, 2013, **13**, 470-474.
- A. S. Arico, P. Bruce, B. Scrosati, J. M. Tarascon and W. Van Schalkwijk, *Nat. Mater.*, 2005, **4**, 366-377.
- X. W. Lou, C. M. Li and L. A. Archer, *Adv. Mater.*, 2009, **21**, 2536-2539.
- X. W. Lou, Y. Wang, C. Yuan, J. Y. Lee and L. A. Archer, *Adv. Mater.*, 2006, **18**, 2325-2329.
- W. S. Kim, Y. Hwa, J. H. Jeun, H. J. Sohn and S. H. Hong, *J. Power Sources*, 2013, **225**, 108-112.
- J. Wang, H. Zhao, X. Liu, J. Wang and C. Wang, *Electrochim. Acta*, 2011, **56**, 6441-6447.
- J. Read, D. Foster, J. Wolfenstine and W. Behl, *J. Power Sources*, 2001, **96**, 277-281.
- X. W. Guo, X. P. Fang, Y. Sun, L. Y. Shen, Z. X. Wang and L. Q. Chen, *J. Power Sources*, 2013, **226**, 75-81.
- X. Chen, K. Kierzek, K. Wilgosz, J. Machnikowski, J. Gong, J. Feng, T. Tang, R. J. Kalenczuk, H. Chen, P. K. Chu and E. Mijowska, *J. Power Sources*, 2012, **216**, 475-481.
- B. P. Vinayan and S. Ramaprabhu, *J. Mater. Chem. A*, 2013, **1**, 3865-3871.
- X. Li, X. Meng, J. Liu, D. Geng, Y. Zhang, M. N. Banis, Y. Li, J. Yang, R. Li, X. Sun, M. Cai and M. W. Verbrugge, *Adv. Funct. Mater.*, 2012, **22**, 1647-1654.
- S. Ding, D. Luan, F. Y. C. Boey, J. S. Chen and X. W. Lou, *Chem. Commun.*, 2011, **47**, 7155-7157.
- Y. Zhu, C. Li and C. Cao, *RSC Adv.*, 2013, **3**, 11860-11868.
- Q. Han, J. Zai, Y. Xiao, B. Li, M. Xu and X. Qian, *RSC Adv.*, 2013, **3**, 20573-20578.
- H. X. Yang, J. F. Qian, Z. X. Chen, X. P. Ai and Y. L. Cao, *J. Phys. Chem. C*, 2007, **111**, 14067-14071.
- Y. J. Hong, M. Y. Son and Y. C. Kang, *Adv. Mater.*, 2013, **25**, 2279-2283.
- S. J. Han, B. C. Jang, T. Kim, S. M. Oh and T. Hyeon, *Adv. Funct. Mater.*, 2005, **15**, 1845-1850.
- W. Wei, Z. Wang, Z. Liu, Y. Liu, L. He, D. Chen, A. Umar, L. Guo and J. Li, *J. Power Sources*, 2013, **238**, 376-387.
- M. Sevilla and A. B. Fuertes, *Chem. Eur. J.*, 2009, **15**, 4195-4203.
- M. Zheng, Y. Liu, K. Jiang, Y. Xiao and D. Yuan, *Carbon*, 2010, **48**, 1224-1233.
- M. Zheng, Y. Liu, Y. Xiao, Y. Zhu, Q. Guan, D. Yuan and J. Zhang, *J. Phys. Chem. C*, 2009, **113**, 8455-8459.
- M. Sevilla and A. B. Fuertes, *Carbon*, 2009, **47**, 2281-2289.
- C. Yao, Y. Shin, L. Q. Wang, C. F. Windisch, Jr., W. D. Samuels, B. W. Arey, C. Wang, W. M. Risen, Jr. and G. J. Exarhos, *J. Phys. Chem. C*, 2007, **111**, 15141-15145.
- P. Manjula, R. Boppella and S. V. Manorama, *ACS Appl. Mat. Interfaces*, 2012, **4**, 6252-6260.
- S. Y. Ho, A. S. W. Wong and G. W. Ho, *Cryst. Growth Des.*, 2009, **9**, 732-736.
- Y. Zhao, J. Li, Y. Ding and L. Guan, *RSC Adv.*, 2011, **1**, 852-856.
- K. Kravchuk, L. Protesescu, M. I. Bodnarchuk, F. Krumeich, M. Yarema, M. Walter, C. Guntlin and M. V. Kovalenko, *J. Amer. Chem. Soc.*, 2013, **135**, 4199-4202.
- S. K. Park, S. H. Yu, N. Pinna, S. Woo, B. Jang, Y. H. Chung, Y. H. Cho, Y. E. Sung and Y. Piao, *J. Mater. Chem.*, 2012, **22**, 2520-2525.
- W. Wang, P. Li, Y. Fu and X. Ma, *J. Power Sources*, 2013, **238**, 464-468.
- K. T. Nam, D. W. Kim, P. J. Yoo, C. Y. Chiang, N. Meethong, P. T. Hammond, Y. M. Chiang and A. M. Belcher, *Science*, 2006, **312**, 885-888.
- X. Wang, X. Zhou, K. Yao, J. Zhang and Z. Liu, *Carbon*, 2011, **49**, 133-139.
- W. Wei, W. Lv, M. B. Wu, F. Y. Su, Y. B. He, B. Li, F. Y. Kang and Q. H. Yang, *Carbon*, 2013, **57**, 530-533.
- R. D. Cakan, M.-M. Titirici, M. Antonietti, G. Cui, J. Maier and Y.-S. Hu, *Chem. Commun.*, 2008, 3759-3761.
- Z. T. Li, G. L. Wu, D. Liu, W. T. Wu, B. Jiang, J. T. Zheng, Y. P. Li, J. H. Li and M. B. Wu, *J. Mater. Chem. A*, 2014, DOI: 10.1039/C4TA00361F.
- Z. Wang, L. Zhou and X. W. Lou, *Adv. Mater.*, 2012, **24**, 1903-1911.

SnO_2/C microspheres and double layered core-shell SnO_2 microspheres can be synthesized in large scale by a facile hydrothermal method followed by heat-treatment. The SnO_2/C microsphere anode of Li-ion batteries exhibits superior rate capability and cyclic stability.

